

ADAPTIVE SCALE ADJUSTMENT DESIGN OF UNSHARP MASKING FILTERS FOR IMAGE CONTRAST ENHANCEMENT

NGAIMING KWOK¹, HAIYAN SHI², GU FANG³, QUANG HA⁴

¹School of Mechanical and Manufacturing Engineering, The University of New South Wales, NSW 2052, Australia

²School of Computer Science and Technology, Shaoxing University, Shaoxing 312000, China

³School of Computing, Engineering and Mathematics, University of Western Sydney, NSW 2751, Australia

⁴School of Electrical, Mechanical and Mechatronic Systems, University of Technology Sydney, NSW 2007, Australia

E-MAIL: nmkwok@unsw.edu.au, csshy@usx.edu.cn, g.fang@uws.edu.au, quang.ha@uts.edu.au

Abstract:

The unsharp masking filter (UMF) has been widely used in image processing front ends for contrast enhancement. The filter, being easy to implement, is based on the concept of augmenting a scaled and high-passed version of the image to itself. The UMF performance is critically dependent on the generation of the high-passed signal to be added as well as its associated scale factor. However, the optimal choice of filter parameters still remains a challenging task due to possible intensity clipping problems where the filtered pixel magnitude is vulnerable to be out of the permitted display ranges. In this research, an adaptive scheme is formulated such that the scale is derived from the pixel intensity of the input image. Specifically, pixels in the mid-range intensity will be assigned a larger scaling factor according to a Gaussian-like profile. In addition, the optimal profile coefficients and the width of the high-pass generator window are determined by adopting the particle swarm optimization algorithm. Satisfactory simulation results obtained from a collection of a large set of images have shown the effectiveness of the proposed image contrast enhancement approach.

Keywords:

Unsharp masking; Adaptive scale adjustment; Kernel design; Particle swarm optimization

1 Introduction

Image processing is a valuable technique used in a wide range of applications. For example, in traffic monitoring, it is required to eliminate shadows in images captured from cameras [1] and extract vehicles from the background scene [2]. Moreover, image processing methods are used in segmenting blood vessels in fundus images [3] to help medical diagnostic. In remote sensing applications, pixel classifications are conducted

[4] to identify land covers. In robotic applications, vision-based tracking is carried out to monitor a moving mobile platform [5].

In the above mentioned successful application examples, image contrast enhancement is often regarded as the front end of the processing pipeline [6]. Among the available methods, frequency histogram based [7] and spatial based [8] approaches are being widely applied. To this end, the unsharp masking filter (UMF) [9] in the latter category, is renowned for its conceptual tractability and implementation simplicity.

The development of unsharp masking filter is motivated by practices in the printing industry where edges around objects are made more striking by superimposing on the edges a high-passed and scaled portion of the object itself [10]. It is noted that, however, the performance of the UMF heavily relies on the quality of the extracted high-pass signal and the magnitude of the scaling. On the other hand, improper choices of filter parameters often degrade the filtering effectiveness. In particular, when the scaling factor is mis-determined, pixel magnitudes of the resultant image may be driven beyond the permissible storage or display limits.

In this research, the choice of UMF parameters is treated as an optimization problem using the image information content as a criterion. While striving for determining the proper parameter values, the particle swarm optimization (PSO) algorithm is employed as the optimizer for its proven solution quality and implementation simplicity [11]. The parameters including the high-pass signal generator window width, scale factor, and mean and variance of the intensity adaptation Gaussian profile, are coded as particles in the PSO algorithm. A modified iteration termination mechanism is also proposed to improve search efficiency. The developed image contrast enhancement method is further tested against the information content criterion.

The rest of the paper is organized as follows. In Section 2, the basics and limitations of current UMF implementation are reviewed. The application of PSO to obtain optimal filter parameters is detailed in Section 3. In Section 4, experiments conducted are described and results are presented. Finally, a conclusion is drawn in Section 5.

2 Unsharp Masking Filter

The essence of an unsharp masking filter is to enlarge the contrast around edges of objects in an image. On one hand, the superimposed signal can be treated as a high-passed version of the image itself. On the other hand, the augmentation may be derived from subtracting the input image by its low-passed version. The latter approach is advantageous that undesirable effects caused by high-passing noisy pixels can be reduced.

Consider an input image $\mathcal{X} = \{x(u, v)\}$, where (u, v) is the pixel coordinate following the raster-scan convention. Here, $u = 1, \dots, U, v = 1, \dots, V$ are the width and height of the image. The filtered output pixel is given by

$$y(u, v) = x(u, v) + \lambda z(u, v), \quad (1)$$

where λ is the scaling factor and $z(u, v)$ is the augmenting signal. Note that if the input is a color image, the intensity is obtained from a color space conversion, for example, converting from the RGB format to the HSV format and extract the V-component as the intensity image.

Let the input image be low-pass filtered by convolving with an averaging kernel. The kernel size is $\omega \times \omega$ pixels. Then the equivalent high-passed signal is

$$z(u, v) = x(u, v) - x(u, v) \otimes \mathcal{A}(\omega), \quad (2)$$

where \otimes is the convolution operator, $\mathcal{A}(\omega)$ is the averaging kernel. When ω is small, the kernel becomes an impulse and the convolved signal will resemble that of the input image. On the contrary, a large ω value will make the kernel to behave as an averaging operator over a large neighborhood. The magnitude of the high-passed signal $z(u, v)$ is hence affected by the choice of the ω . Consequently, the UMF performance crucially relies on a proper selection of the ω value.

An example case is now presented to illustrate the importance of choosing optimal UMF parameters on its performance. If the storage or display device accepts only applied magnitudes in $[0, 1]$, then the filtered output image must be confined. That is, we have to ensure that $y(u, v) \in [0, 1]$ as required. Furthermore, it is noticed that the input is also limited within $[0, 1]$ in most systems in practice. Hence, there is always a non-zero

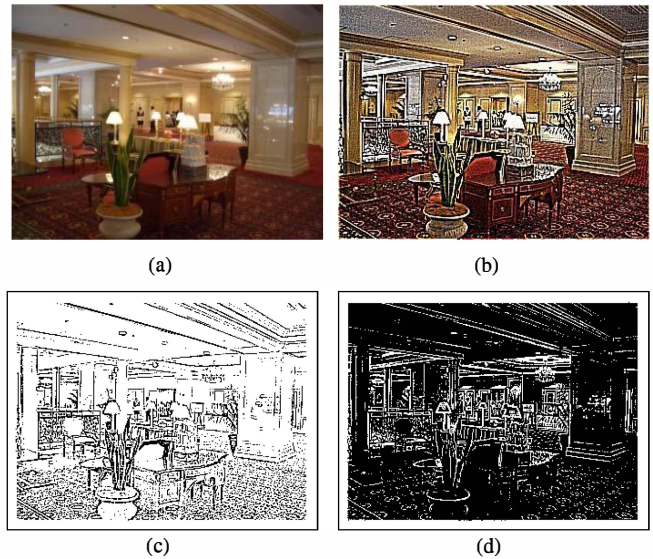


Figure 1. Over-range phenomenon; (a) input image, (b) filtered image, (c) pixels of $y(u, v) < 0$ (black), (d) pixels of $y(u, v) > 1$ (white).

probability that the addition of the enhancement term $\lambda z(u, v)$ may cause the output pixel magnitude to rest beyond the allowable display range. That is, when $y(u, v) < 0$ or $y(u, v) > 1$, the displayed image may not truly represent the correct information contained in the scene. Hence, it is a critical issue that the gain factor λ has to be properly determined.

Figure 1 illustrates the over-range phenomenon of a typical indoor image (Fig. 1(a)). The kernel width and scale factor are arbitrarily set to $\omega = 3, \lambda = 30$, and the unsharp masking process is conducted. It can be seen in Fig. 1(b) that the over-range phenomenon is evident where the output image appears unnatural. Pixels whose magnitudes are below zero are shown in Fig. 1(c) while those above unity are shown in Fig. 1(d). This example has clearly indicated that an optimal choice of the scale factor is necessary to obtain a satisfactory filtered image as shown below.

The effect of the low-pass kernel parameter, ω , on the UMF performance is illustrated in Fig. 2. In figures 2(a) and 2(b), the resultant over-range phenomenon from small neighborhood size, $\omega = 1$ and $\lambda = 5$, is depicted. For a large neighborhood size, $\omega = 10$ and $\lambda = 5$, the phenomenon is illustrated in figures 2(c) and 2(d). A careful inspection will reveal that for different averaging kernel parameters, the over-range phenomenon is more severe for the larger ω value.

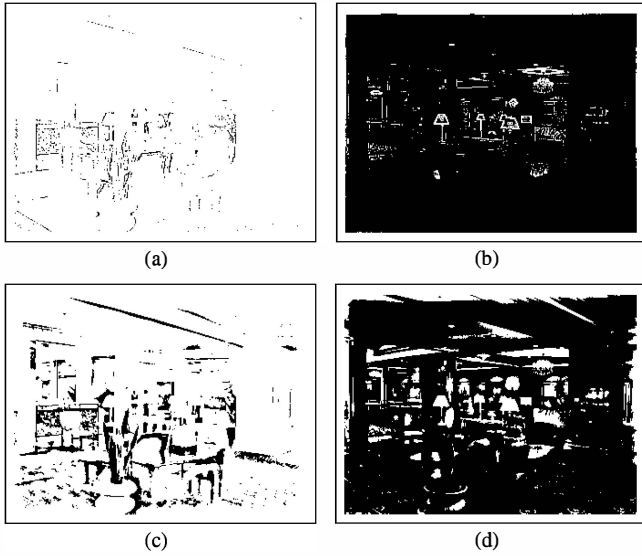


Figure 2. Influence of low-pass kernel parameter; (a) pixels below zero (black), $\omega = 1$, (b) pixels above unity (white), $\omega = 1$, (c) pixels below zero (black), $\omega = 10$, (d) pixels above unity (white), $\omega = 10$.

The above example has revealed that the choices of the scale factor λ and averaging kernel size ω are crucial to the performance of the UMF. Moreover, the effects of these parameters on the filtered results are inter-related. In order to alleviate the over-range problem, the scale factor λ is made adaptive to the local pixel magnitude $x(u, v)$. The development of the adaptive scheme is presented below.

Consider a general pixel in the input image $x(u, v)$, its magnitude will be added with the scaled and high-passed value $\lambda z(u, v)$ from the UMF operation. Here, we propose to adjust λ in accordance to a Gaussian-like profile

$$\lambda(u, v) = \exp \left\{ \frac{-(x(u, v) - \mu)^2}{2\sigma^2} \right\}, \quad (3)$$

where $\mu \in [0, 1]$ is the center of the adjustment profile, $\sigma > 0$ is the standard deviation of the Gaussian profile. That is, we have now

$$\lambda \leftarrow k\lambda(u, v, x(u, v)), \quad (4)$$

where k is the multiplicative gain factor compensating for $\max(\lambda(u, v, x(u, v))) = 1$. By using this profile, pixels having intensities in the mid-range intensity will receive a higher augmentation of the high-passed signal to enhance the contrast.

On the other hand, when the pixel intensity rests on the low- or high-range regions, the particular pixel will receive reduced scalings. By reducing the augmentation magnitude, the over-range problem could be alleviated.

An example case is tested against different settings of μ and σ and the over-range phenomena are indicated in Fig. 3. In the tests, we have set $\omega = 3$, $k = 15$ as constants. It is observed from the figure that the adjustment profile $\lambda(u, v, x(u, v))$ with different parameter settings are affecting the UMF performance. In particular, for large σ in tests 2 and 4, the output has a larger number of over-range pixels.

The motivation for employing adaptive scaling and the effect of the filter parameters on the UMF performance have been demonstrated. It is obvious that proper parameter settings are necessary in order to obtain satisfactory image contrast enhancements. In the following section, the use of the particle swarm optimization algorithm for determining optimal parameters will be described.

3 Particle Swarm Optimization

Potential solutions for UMF parameters in the particle swarm optimization (PSO) algorithm are coded into a vector representation called a particle. The PSO iterative procedure can be described by the following expressions,

$$\mathbf{v}_{t+1}^i = w^i \mathbf{v}_t^i + c_g^i (\mathbf{g}_{best,t} - \mathbf{x}_t^i) + c_p^i (\mathbf{p}_{best,t}^i - \mathbf{x}_t^i), \quad (5)$$

$$\mathbf{x}_{t+1}^i = \mathbf{x}_t^i + \mathbf{v}_{t+1}^i, \quad (6)$$

where \mathbf{x}^i is the problem dependent d -dimensional particle position in the solution space, i is the particle index, $i = 1, \dots, P$, \mathbf{v}^i is the velocity of the particle movement assuming a unity time step, w^i is the velocity control coefficient, c_g^i , c_p^i are random gain control variables, \mathbf{g}_{best} is the global-best position, \mathbf{p}_{best}^i is the position of a particular particle corresponding to its problem dependent best objective obtained so far. Subscript t is the iteration index. Typical parameter values, such as $w = 0.6$, c_g^i , $c_p^i \in [0, 1]$ are used in the experiments.

At the start of the algorithm, the particle positions \mathbf{x}_0^i are randomly assigned to cover the solution space. A problem dependent objective function, acting as the fitness of a particle, is evaluated and assigned to each particle. Based on the set of objective values, the particle having the highest (lowest) fitness for a maximization (minimization) problem is taken as the global-best $\mathbf{g}_{best,0}$. This set of initial objective values is denoted as the particle-best $\mathbf{p}_{best,0}^i$. The velocity is then calculated using some random gain coefficients (c_g^i , c_p^i) usually sampled from a uniform distribution. The particle positions

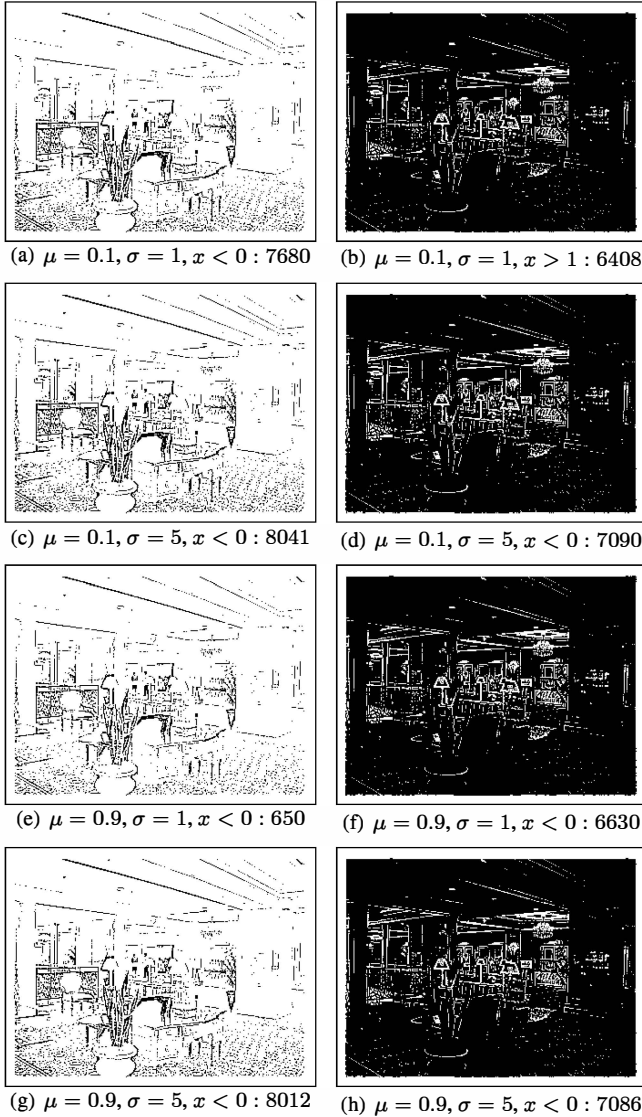


Figure 3. Demonstration of the effect of adjustment profile parameters; left column - pixel intensities less than zero (black), right column - pixel intensities greater than unity (white).

are updated according to Equ. (6) and then the procedure repeats. Finally, at the satisfaction of some termination criteria, the global-best particle is reported as the solution to the problem.

In the optimization of UMF parameters, we code the variables as a particle

$$\mathbf{x} = [\omega \ k \ \mu \ \sigma]^T. \quad (7)$$

The objective function to be maximized is the information content, Shannon's entropy, contained in the filtered image.

$$\mathcal{H} = - \sum p_i \log p_i, \quad i = 0, \dots, 255 \quad (8)$$

where p_i is the probability that a pixel intensity falls within one of the 256 intensity regions for a 8-bit digital image. In addition, in order to search for optimal parameters for minimum over-range artifacts, the entropy is combined with a penalty component, giving

$$\theta = \mathcal{H} \times \left(1 - \frac{\eta}{U \times V}\right), \quad (9)$$

where η is the number of over-range pixels, $U \times V$ is the total number of pixels in the image. If there is a large number of pixels falling outside the permitted display range, then θ will decrease and signify a less optimal solution. With regard to the PSO termination condition, we use the following procedure described in Algorithm 1.

Algorithm 1 PSO Iteration Procedure

- 1: set iteration count $m = 0$, no-improve count $n = 0$;
 - 2: **repeat**
 - 3: conduct PSO procedure, Equ. (5), (6);
 - 4: if $\theta_o < \theta_i$, advance no-improve count $n = n + 1$;
 - 5: advance iteration count $m = m + 1$;
 - 6: **until** $m - n > \gamma$.
-

In the algorithm θ_i and θ_o are the objective functions of the input and filtered images respectively. The termination coefficient γ is set at 10 ensuring that there is an improvement on the filtered image contrast for at least 10 iterations.

4 Experiment

Experiments are conducted to verify the effectiveness of the proposed adaptive unsharp masking method for image contrast enhancement. A collection of 24 colour images from benchmark photographs obtained from <http://r0k.us/graphics/kodak/index.html>, together with 76

additional images taken by the authors in indoor and outdoor environments are used. Because of the differences in the feature characteristics in individual images, the output image from the UMF may contain a diversified improvement in the information content. Example images of various entropy increments are shown below.

In Fig. 4, the image has obtained a relative highest gain among the test images. In particular, it is noted that the input image have a low entropy, as the image appears blurry due to imperfections during the image acquisition process imposed by the environment.

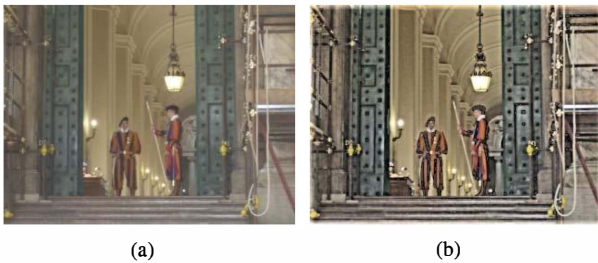


Figure 4. Filtered image with highest gain in entropy (0.722); (a) input image, (b) filtered image.

Figure 5 depicts the input image and the filtered version. The improvement in contrast is high where the image features a flat surface with a few objects. In particular, the image is occupied with a large portion of similar color tone. Nonetheless, the UMF method is able to provide contrast enhancement.



Figure 5. Filtered image with higher gain (0.435); (a) input image, (b) filtered image.

An image of outdoor scene and its enhanced result from the UMF are shown in Fig. 6. The image contains a mixture of color tones and a wide depth of view. The original image has already a high entropy and the gain in information is the average within the set of test images.



Figure 6. Filtered image with average gain (0.093); (a) input image, (b) filtered image.

The statistics of the 100 test image results are presented in Fig. 7. The relative gain in entropy is plotted in Fig. 7(a) where it can be seen that the resultant entropies are above the diagonal line. This indicates that contrast enhancements are available from the proposed adaptive UMF approach. In Fig. 7(b), the distribution of information gains is plotted and the average improvement is 0.095.

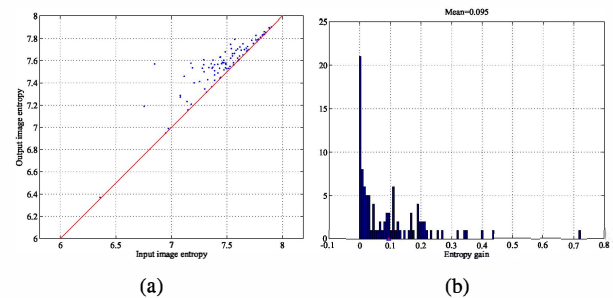


Figure 7. Gain in entropy; (a) comparison between input and filtered images, (b) distribution of entropy gain.

The distributions of the filter parameters are also depicted. In Fig. 8(a), it is shown that the averaging kernel width peaks at 11 which is a realistic value that amounts to about 2 ~ 3% of the image width. The gain factor, magnifying the high-passed component to be augmented to the input image, takes on the value of 1.395. This value, however, is regarded as problem dependent and a challenge in UMF design if the optimization approach is not adopted. Figures 8(c) and 8(d) contain the distributions of the Gaussian profile in adapting the intensity to the augmentation magnitude. The mean settles on 0.409 and the standard deviation is 0.424. It can be envisioned that pixels whose intensities are at the low end or high end are receiving

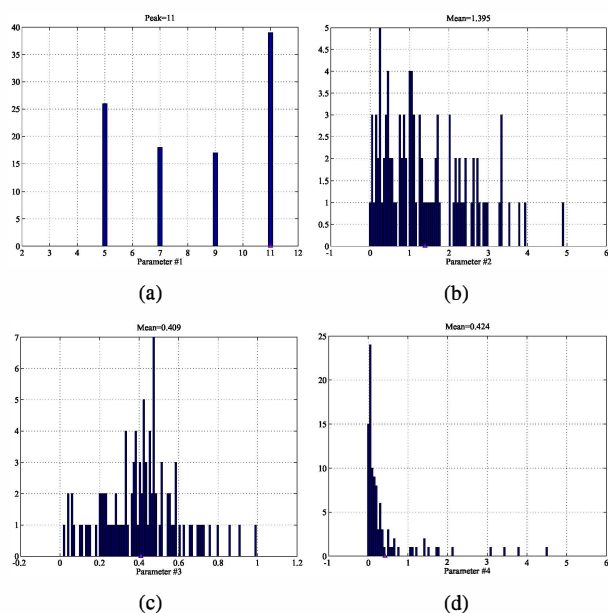


Figure 8. Statistics of filter parameter values; (a) averaging kernel width ω , (b) gain k , (c) Gaussian kernel mean value μ , (d) Gaussian kernel standard deviation σ .

smaller magnifications as those pixels in the mid-intensities. This observation verifies the validity of the proposed adjustment scheme.

5 Conclusion

An adaptive gain adjustment approach has been proposed for image contrast enhancement using an unsharp masking filter. A Gaussian-like profile is designed, where larger gains are allocated to mid-range intensity pixels, in order to avoid drawbacks imposed from the over-range phenomenon as found in the case of constant scaling. Furthermore, the determination of optimal filter parameters is realized by the use of the particle swarm optimization algorithm. Satisfactory contrast enhancement results are obtained and the effectiveness of the developed method is verified. Moreover, statistics from experimental results are provided as recommendations for future filter designs.

References

[1] J. T. Xue, L. Y. Hui, and S. F. Xing, "Research on shadow elimination in intelligent traffic monitoring," in

Proc. 2012 International Conference on Machine Learning and Cybernetics, 2012, pp. 1350–1355.

[2] S. Y. Chen, J. H. Zhang, Y. F. Li, and J. W. Zhang, "A hierarchical model incorporating segmented regions and pixel descriptors for video background subtraction," *IEEE Transactions on Industrial Informatics*, vol. 8, no. 1, pp. 118–127, 2012.

[3] F. L. Yi and W. H. Xu, "Segmentation of blood vessels in color fundus images based on optimal multi-threshold method," in Proc. 2012 International Conference on Machine Learning and Cybernetics, 2012, pp. 725–728.

[4] G. Zhang, X. Jia, and N. M. Kwok, "Spectral-spatial based super pixel remote sensing image classification," in Proc. 2011 4th International Congress on Image and Signal Processing, 2011, pp. 1680–1684.

[5] Y. H. Yu, N. M. Kwok, and Q. P. Ha, "Color tracking for multiple robot control using a system-on-programmable-chip," *Automation in Construction*, vol. 20, pp. 669–676, 2011.

[6] P. Milanfar, "A tour of modern image filtering: New insights and methods, both practical and theoretical," *IEEE Signal Processing Magazine*, vol. 30, no. 1, pp. 106–128, 2013.

[7] N. M. Kwok, X. Jia, D. Wang, S. Y. Chen, G. Fang, and Q. P. Ha, "Visual impact enhancement via image histogram smoothing and continuous intensity relocation," *Computers and Electrical Engineering*, vol. 37, no. 5, pp. 681–694, 2011.

[8] H. Shi, "Determination of bilateral filter coefficients based on particle swarm optimization," in Proc. 2012 5th International Congress on Image and Signal Processing, 2012, pp. 302–306.

[9] C. L. D. A. Mai, M. T. T. Nguyen, and N. M. Kwok, "A modified unsharp masking method using particle swarm optimization," in Proc. 4th International Congress on Image and Signal Processing, 2011, pp. 646–650.

[10] G. Deng, "A generalized unsharp masking algorithm," *IEEE Transactions on Image Processing*, vol. 20, no. 5, pp. 1249–1261, 2011.

[11] F. van den Bergh and A. Engelbrecht, "A cooperative approach to particle swarm optimization," *IEEE Transactions on Evolutionary Computation*, vol. 8, no. 3, pp. 225–239, 2004.